21

Active Vibration Control of a Smart Beam by Using a Spatial Approach

Ömer Faruk KIRCALI[1, 2], Yavuz YAMAN[2],
Volkan NALBANTOĞLU[2] and Melin ŞAHİN[2]
[1]*STM Savunma Teknolojileri Muhendislik ve Ticaret A.S., Ankara, TURKIYE*
[2]*Department of Aerospace Engineering, Middle East Technical University, Ankara, TURKIYE*

1. Introduction

The vibration control is an important and rapidly developing field for lightweight flexible aerospace structures. Those structures may be damaged or become ineffective under the undesired vibrational loads they constantly experience. Hence, they require effective control mechanism to attenuate the vibration levels in order to preserve the structural integrity. The usage of smart materials, as actuators and/or sensors, has become promising research and application area that gives the opportunity to accomplish the reduction of vibration of flexible structures and proves to be an effective active control mechanism.

For the last few decades there has been an extensive research about the piezoelectric materials because of the capability of being used both as actuators and sensors. The smart structure is a structure that can sense external disturbance and respond to that in real time to fulfil operational requirements. Smart structures consist of passive structure, highly distributed active devices called smart materials/elements and processor networks. The smart materials are primarily used as sensors and/or actuators and are either embedded or attached to an existing passive structure (Çalışkan, 2002). Today, the main and maybe the most widespread application area of piezoelectric materials is using them as collocated actuator and sensor pair for active vibration control purposes (Prasad, 1998).

Active vibration control of a smart structure starts with an accurate mathematical model of the structure. Modeling smart structures may require the modeling of both passive structure and the active parts. Crawley and de Luis (1989), by neglecting the mass of active elements, presented an analytical modeling technique to show that the piezoelectric actuators can be used to suppress some modes of vibration of a cantilevered beam. Similar approach was carried out on thin plates by Dimitridis et al (1991). Although neglecting the mass and stiffness properties of the smart materials compared to the passive structure is generally acceptable, the modeling of a smart structure mainly involves the force and moment descriptions generated by the smart materials. Sample modeling studies are proposed by

several researchers such as Pota et al. (1992), Halim (2002b) The governing differential equations of motion of the smart structures can then be solved by analytical methods, such as modal analysis, assumed-modes method, Galerkin's method or finite element method (Meirovitch, 1986).

Since it is not so easy to consider all non-uniformities in structural properties of a smart structure, the analytical modeling techniques such as finite element model, modal analysis or assumed modes method allow one to obtain system model including only the approximate information of optimal placement of piezoelectric patches, natural frequencies and mode shapes of the structure except damping (Çalışkan, 2002 and Halim, 2002b). In order to improve the model, Nalbantoğlu (1998) and Nalbantoğlu et al. (2003) showed that experimental system identification techniques can be applied on flexible structures and they may help one to identify the system more accurately.

Due to having a large number of resonant modes, the high frequency characteristics of a flexible structure generally cause problems in identifying the system method. Since, usually the first few vibrational modes are taken into account in the controller design, the reduction of the model is often required to obtain the finite-dimensional system model (Hughes, 1981; Balas, 1995 and Moheimani, 1997). General approach for reducing the order of the model is the direct model reduction. However, removing the higher modes directly from the system model perturbs zeros of the system (Clark, 1997). Minimizing the effect of model reduction and correcting the system model is possible by adding a feedthrough, or correction, term including some of the removed modes, to the truncated model (Clark, 1997; Moheimani, 2000d and Moheimani, 2000c). Halim (2002b) proposed an optimal expression for feedthrough term in case of undamped and damped system models.

Various control techniques have been used as active control strategy like optimal control (Hanagoud, 1992), LQG control (Bai, 1996) and robust control using H_∞ (Nalbantoğlu, 1998; Yaman, 2001 and Ülker, 2003) or H_2 control framework (Halim, 2002c). The H_∞ control design technique for robust control phenomena has been developed by many researchers for various application areas including the vibration control (Zames, 1981; Francis, 1984; Doyle, 1989 and Lenz, 1993). Yaman et al. (2001, 2003b) showed the effect of H_∞ based controller on suppressing the vibrations of a smart beam due its first two flexural modes. They also extended their studies to a smart plate (2002a, 2002b). Ülker (2003) showed that, besides the H_∞ control technique, μ-synthesis based controllers can also be used to suppress vibrations of smart structures. In all those works on flexible structures, the general control strategy focused on analyzing the vibrations at specific locations over the structure and minimizing them. However, that kind of pointwise controller design ignores the effect of vibration at the rest of the body and a successful vibration reduction over entire structure can not always be accounted for.

Moheimani and Fu (1998c) introduced spatial H_2 norm, which is a measured performance over spatial domain, for spatially distributed systems in order to meet the need of spatial vibration control. Besides, Moheimani et al. (1997, 1998a) proposed spatial H_∞ norm

concept and simulation based results of spatial vibration control of a cantilevered beam were presented. Moheimani et al. (1998b, 1999) carried out the spatial approach on feedforward and feedback controller design, and presented illustrative results. They also showed that spatial H_∞ controllers could be obtained from standard H_∞ controller design techniques. Although the simulations demonstrated successful results on minimizing the vibrations over entire beam, implementation of that kind of controllers was not guaranteed on real world systems. Halim (2002b, 2002c) studied the implementation of spatial H_2 controllers on active vibration control of a simply-supported beam experimentally and presented successful results. He continued to work on simply-supported beams about implementation of spatial H_∞ controller and obtained successful experimental results (Halim, 2002a). Further experimental studies were performed on active vibration control of a simply-supported piezoelectric laminate plate by Lee (2005). Lee also attenuated acoustic noise due to structural vibration.

The current chapter aims to summarize the studies of modelling and spatial control of a cantilevered beam (Kırcalı et al. 2008, 2007, 2006a and 2006b).

2. Assumed-Modes Modeling of the Smart Beam

Consider the cantilevered smart beam model used in the study which is depicted in Fig.1. The smart beam consists of a passive aluminum beam (507mmx51mmx2mm) with eight symmetrically surface bonded SensorTech BM500 type PZT (Lead-Zirconate-Titanate) patches (25mmx20mmx0.5mm), which are used as the actuators. Note that, in this study, the group of PZT patches on one side of the beam is considered as if it is a single patch. The beginning and end locations of the PZT patches along the length of the beam away from the fixed end are denoted as r_1 and r_2, and the patches are assumed to be optimally placed (Çalışkan, 2002). The subscripts *b*, *p* and *sb* indicate the passive beam, PZT patches and smart beam respectively. Analytical modeling of the smart beam is performed by assumed-modes method, which represents the deflection of the beam by means of a series solution:

$$y(r,t) = \sum_{i=1}^{N} \phi_i(r) q_i(t) \tag{1}$$

where ϕ_i are admissible functions which satisfy the geometric boundary conditions of the passive beam, q_i are time-dependent generalized coordinates, *r* is the longitudinal axis and *t* is time. Assumed-modes method uses this solution to obtain approximate system model of the structure with the help of energy expressions (Mason, 1981). The kinetic and potential energies of the smart beam can be determined to be (Kırcalı, 2006a):

$$T_{sb}(t) = \frac{1}{2} \sum_{i=1}^{N} \sum_{j=1}^{N} \left\{ \int_0^{L_b} \rho_b A_b \phi_i \phi_j dr + 2 \int_{r_1}^{r_2} \rho_p A_p \phi_i \phi_j dr \right\} \dot{q}_i \dot{q}_j \tag{2}$$

$$V_{sb}(t)=\frac{1}{2}\sum_{i=1}^{N}\sum_{j=1}^{N}\left\{\int_{0}^{L_b}E_bI_b\phi_i''\phi_j''dr+2\int_{r_1}^{r_2}E_pI_p\phi_i''\phi_j''dr\right\}q_iq_j \tag{3}$$

The total viscous damping force of the smart beam can similarly be obtained as (Kırcalı, 2006a):

$$F_{sb}=\frac{1}{2}\sum_{i=1}^{N}\sum_{j=1}^{N}\left\{\int_{0}^{L_b}(2\xi_i\omega_i)\rho_bA_b\phi_i\phi_jdr+2\int_{r_1}^{r_2}(2\xi_i\omega_i)\rho_pA_p\phi_i\phi_jdr\right\}\dot{q}_i\dot{q}_j \tag{4}$$

where the beam's density, Young's modulus of elasticity, second moment of area and cross sectional area are defined as ρ_b, E_b, I_b, and A_b respectively. Also note that subscript *i* and *j* yield number of eigenvalues, ξ_i is the viscous damping coefficient of the i^{th} mode and ω_i represents the i^{th} natural frequency of the beam.

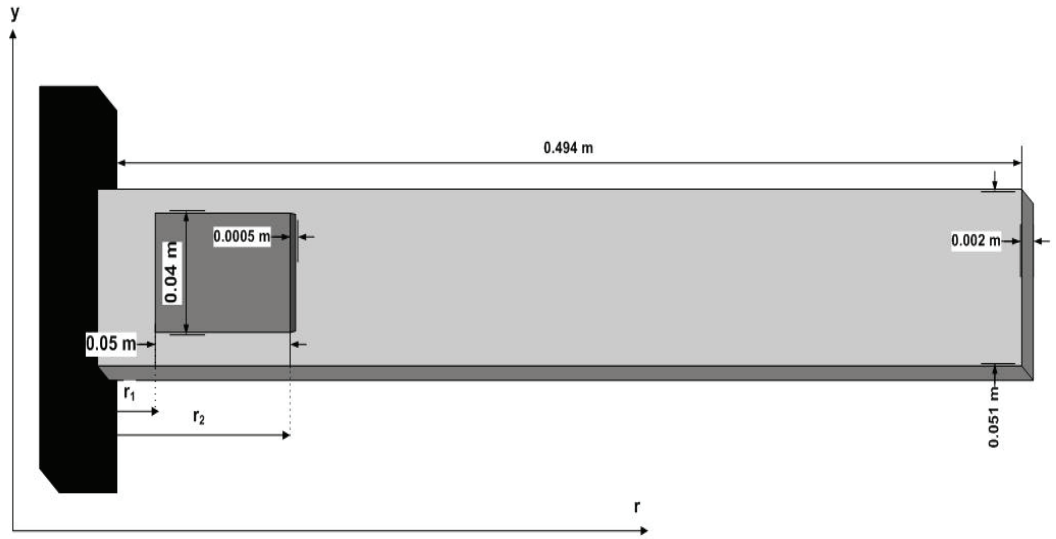

Fig. 1. The smart beam model used in the study

The PZT patches are placed in a collocated manner and the voltage is applied in order to create a bimorph configuration (PZT patches bonded to opposite faces of the beam have opposite polarity), the resulting effect on the beam becomes equivalent to that of a bending moment. This case is shown in Fig.2:

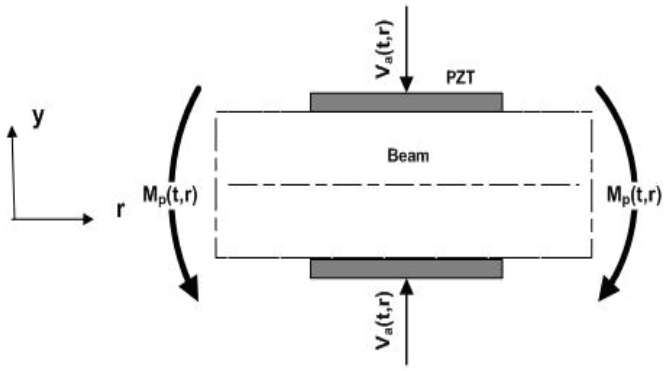

Fig. 2. Inducing bending moment by applying voltage to PZT patches

Here $M_p(t,r)$ denotes the bending moment and $V_a(t,r)$ is the applied voltage. When the voltage is applied on a PZT patch, a piezoelectric strain ε_p is introduced in the patch (Baz, 1988):

$$\varepsilon_p(t,r) = \frac{d_{31}}{t_p} V_a(t,r) \tag{5}$$

The longitudinal stress consequently generates a bending moment about the neutral axis of the system, as:

$$M_p(t,r) = C_p V_a\left(t,r\right) \tag{6}$$

where C_p is a geometric constant due to bending moment, and expressed as:

$$C_p = E_p d_{31} w_p (t_p + t_b) \tag{7}$$

As a consequence, the transfer function, $G_N(s,r)$, from the input voltage to the beam deflection in the frequency domain, including *N* number of eigenfunctions, is obtained as:

$$G_N(s,r) = \sum_{i=1}^{N} \frac{\overline{P}_i \phi_i(r)}{s^2 + 2\xi_i \omega_i s + \omega_i^2} \tag{8}$$

where

$$\overline{P}_i = \frac{C_p\left[\phi_i'(r_2) - \phi_i'(r_1)\right]}{\left\{\rho A L^3\right\}_{sb}} \tag{9}$$

and

$$\left\{\rho A L^3\right\}_{sb} = \rho_b A_b L_b^3 + 2\rho_p A_p L_p^3 \tag{10}$$

The detailed derivation of equation (8) can be found in (Kırcalı, 2006a). In this study, the assumed modes (i.e. the admissible functions) of the fixed-free smart beam are taken as the eigenfunctions of the fixed-free passive beam:

$$\phi_i(r) = L_b\left\{\cosh\beta_i r - \cos\beta_i r - \frac{\cos\beta_i L_b + \cosh\beta_i L_b}{\sin\beta_i L_b + \sinh\beta_i L_b}\left(\sinh\beta_i r - \sin\beta_i r\right)\right\} \tag{11}$$

3. Model Correction and Spatial Identification of the Smart Beam

Assumed-modes method uses admissible functions in order to model the dynamics of the system, but ignores the nonuniform mass and stiffness distributions. If one uses a large number of admissible functions, or more general if their number goes to infinity, the model will be exactly the same as the original one. However, using infinite number of admissible functions is not convenient to apply for real structures at least for huge amount of computing requirements. Therefore, it is generally believed that the utilization of sufficiently large number of admissible functions will be enough to increase the accuracy of the approximate system model (Hughes, 1987).

Including large number of admissible functions leads to not only a more accurate but also a high order approximate system model. Since the order of an H_∞ controller depends on the system order , such a higher order model yields an excessive order controller which may not be possibly implemented. However, the controller design techniques generally focus on a particular bandwidth which includes only a few vibration modes of the system. In this respect, the reduction of the order of the model is required.

One of the most popular techniques for reducing the order of the system model is the direct model reduction, which simplifies the system model by directly truncating the higher modes of frequency range of interest. However, removing the higher modes may perturb the zeros of the system which will affect the closed-loop performance and stability (Clark, 1997). One particular approach to compensate the error of the model truncation was

presented by Moheimani (Moheimani, 2000a) which considers adding a correction term that minimizes the weighted spatial H_2 norm of the truncation error. The additional correction term had a good improvement on low frequency dynamics of the truncated model. Moheimani (2000d) and Moheimani et al. (2000c) developed their corresponding approach to the spatial models which are obtained by different analytical methods. Moheimani (2006b) presented an application of the model correction technique on a simply-supported piezoelectric laminate beam experimentally. However, in all those studies, the damping in the system was neglected. Halim (2002b) improved the model correction approach with damping effect in the system. This section will give a brief explanation of the model correction technique with damping effect based on those previous works (Moheimani, 2000a, 2000c and 2000d) and for more detailed explanation the reader is advised to refer to the reference (Moheimani, 2003).

Recall the transfer function of the system from system input to the beam deflection including *N* number of modes given in equation (8). The spatial system model expression includes *N* number of resonant modes assuming that *N* is sufficiently large. The controller design however interests in the first few vibration modes of the system, say *M* number of lowest modes. So the truncated model including first *M* number of modes can be expressed as:

$$G_M(s,r) = \sum_{i=1}^{M} \frac{\bar{P}_i \phi_i(r)}{s^2 + 2\xi_i \omega_i s + \omega_i^2} \tag{12}$$

where $M << N$. This truncation may cause error due to the removed modes which can be expressed as an error system model, $E(s,r)$:

$$\begin{aligned} E(s,r) &= G_N(s,r) - G_M(s,r) \\ &= \sum_{i=M+1}^{N} \frac{\bar{P}_i \phi_i(r)}{s^2 + 2\xi_i \omega_i s + \omega_i^2} \end{aligned} \tag{13}$$

In order to compensate the model truncation error, a correction term should be added to the truncated model (Halim, 2002b):

$$G_C(s,r) = G_M(s,r) + K(r) \tag{14}$$

where $G_C(s,r)$ and $K(r)$ are the corrected transfer function and correction term, respectively.

The correction term $K(r)$ involves the effects of removed modes of the system on the frequency range of interest, and can be expressed as:

$$K(r) = \sum_{i=M+1}^{N} \phi_i(r) k_i \tag{15}$$

where k_i is a constant term. The reasonable value of k_i should be determined by keeping the difference between $G_N(s,r)$ and $G_C(s,r)$ to be minimum, i.e. corrected system model should approach more to the higher ordered one given in equation (8). Moheimani (2000a) represents this condition by a cost function, J, which describes that the spatial H_2 norm of the difference between $G_N(s,r)$ and $G_C(s,r)$ should be minimized:

$$J = << W(s,r)\{G_N(s,r) - G_C(s,r)\} >>_2^2 \tag{16}$$

The notation $<< .. >>_2^2$ represents the spatial H_2 norm of a system where spatial norm definitions are given in (Moheimani, 2003). $W(s,r)$ is an ideal low-pass weighting function distributed spatially over the entire domain R with its cut-off frequency ω_c chosen to lie within the interval (ω_M, ω_{M+1}) (Moheimani, 2000a). That is:

$$\left|W(j\omega, r)\right| = \left\{ \begin{matrix} 1 & -\omega_c < \omega < \omega_{c+1},\ r \in R \\ 0 & elsewhere \end{matrix} \right\}$$
$$and\ \ \omega_c \in (\omega_M, \omega_{M+1}) \tag{17}$$

where ω_M and ω_{M+1} are the natural frequencies associated with mode number M and $M+1$, respectively. Halim (2002b) showed that, by taking the derivative of cost function J with respect to k_i and using the orthogonality of eigenfunctions, the general optimal value of the correction term, so called k_i^{opt}, for the spatial model of resonant systems, including the damping effect, can be shown to be:

$$k_i^{opt} = \frac{1}{4\omega_c\omega_i} \frac{1}{\sqrt{1-\xi_i^2}} \ln\left\{ \frac{\omega_c^2 + 2\omega_c\omega_i\sqrt{1-\xi_i^2} + \omega_i^2}{\omega_c^2 - 2\omega_c\omega_i\sqrt{1-\xi_i^2} + \omega_i^2} \right\} \overline{P_i} \tag{18}$$

An interesting result of equation (18) is that, if damping coefficient is selected as zero for each mode, i.e. undamped system, the resultant correction term is equivalent to those given

in references (Moheimani, 2000a, 2000c and 2000d) for an undamped system. Therefore, equation (18) can be represented as not only the optimal but also the general expression of the correction term.

So, following the necessary mathematical manipulations, one will obtain the corrected system model including the effect of out-of-range modes as:

$$G_C(s,r) = \sum_{i=1}^{M} \frac{\bar{P}_i \phi_i(r)}{s^2 + 2\xi_i \omega_i s + \omega_i^2} + \sum_{i=M+1}^{N} \phi_i(r) \left\{ \frac{1}{4\omega_c \omega_i} \frac{1}{\sqrt{1-\xi_i^2}} \ln \left\{ \frac{\omega_c^2 + 2\omega_c \omega_i \sqrt{1-\xi_i^2} + \omega_i^2}{\omega_c^2 - 2\omega_c \omega_i \sqrt{1-\xi_i^2} + \omega_i^2} \right\} \bar{P}_i \right\} \quad (19)$$

Consider the cantilevered smart beam depicted in Fig.1 with the structural properties given at Table 1. The beginning and end locations of the PZT patches $r_1 = 0.027m$ and $r_2 = 0.077m$ away from the fixed end, respectively. Note that, although the actual length of the passive beam is 507mm, the effective length, or span, reduces to 494mm due to the clamping in the fixture.

	Aluminum Passive Beam	**PZT**
Length	$L_b = 0.494m$	$L_p = 0.05m$
Width	$w_b = 0.051m$	$w_p = 0.04m$
Thickness	$t_b = 0.002m$	$t_p = 0.0005m$
Density	$\rho_b = 2710kg/m^3$	$\rho_p = 7650kg/m^3$
Young's Modulus	$E_b = 69GPa$	$E_p = 64.52GPa$
Cross-sectional Area	$A_b = 1.02 \times 10^{-4} m^2$	$A_p = 0.2 \times 10^{-4} m^2$
Second Moment of Area	$I_b = 3.4 \times 10^{-11} m^4$	$I_p = 6.33 \times 10^{-11} m^4$
Piezoelectric charge constant	-	$d_{31} = -175 \times 10^{-12} m/V$

Table 1. Properties of the Smart Beam

The system model given in equation (8) includes *N* number of modes of the smart beam, where as *N* gets larger, the model becomes more accurate. In this study, first 50 flexural resonance modes are included into the model (i.e. *N=50*) and the resultant model is called *the full order model*:

$$G_{50}(s,r)=\sum_{i=1}^{50}\frac{\overline{P}_i\phi_i(r)}{s^2+2\xi_i\omega_i s+\omega_i^2} \tag{20}$$

However, the control design criterion of this study is to suppress only the first two flexural modes of the smart beam. Hence, the full order model is directly truncated to a lower order model, including only the first two flexural modes, and the resultant model is called *the truncated model*:

$$G_{2}(s,r)=\sum_{i=1}^{2}\frac{\overline{P}_i\phi_i(r)}{s^2+2\xi_i\omega_i s+\omega_i^2} \tag{21}$$

As previously explained, the direct model truncation may cause the zeros of the system to perturb, which consequently affect the closed-loop performance and stability of the system considered (Clark, 1997). For this reason, the general correction term, given in equation (18), is added to the truncated model and the resultant model is called *the corrected model*:

$$\begin{aligned} G_C(s,r)=&\sum_{i=1}^{2}\frac{\overline{P}_i\phi_i(r)}{s^2+2\xi_i\omega_i s+\omega_i^2} \\ &+\sum_{i=3}^{50}\phi_i(r)\left\{\frac{1}{4\omega_c\omega_i}\frac{1}{\sqrt{1-\xi_i^2}}\ln\left\{\frac{\omega_c^2+2\omega_c\omega_i\sqrt{1-\xi_i^2}+\omega_i^2}{\omega_c^2-2\omega_c\omega_i\sqrt{1-\xi_i^2}+\omega_i^2}\right\}\overline{P}_i\right\} \end{aligned} \tag{22}$$

where the cut-off frequency, based on the selection criteria given in equation (17), is taken as:

$$\omega_c=\left(\omega_2+\omega_3\right)/2 \tag{23}$$

The assumed-modes method gives the first three resonant frequencies of the smart beam as shown in Table 2. Hence, the cut-off frequency becomes 79.539 Hz. The performance of model correction for various system models obtained from different measurement points along the beam is shown in Fig.3 and Fig.4.

Resonant Frequencies	Value (Hz)
ω_1	6.680
ω_2	41.865
ω_3	117.214

Table 2. First three resonant frequencies of the smart beam

The error between full order model-truncated model, and the error between full order model-corrected model, so called the error system models $\overline{E}_{F-T}$ and $\overline{E}_{F-C}$, allow one to see the effect of model correction more comprehensively.

$$\overline{E}_{F-T} = G_N(s,r) - G_M(s,r) \tag{24}$$

$$\overline{E}_{F-C} = G_N(s,r) - G_C(s,r) \tag{25}$$

The frequency responses of the error system models are shown in Fig.5 and Fig.6. One can easily notice from the aforementioned figures that, the error between the full order and corrected models is less than the error between the full order and truncated ones in a wide range of the interested frequency bandwidth. That is, the model correction minimizes error considerably and makes the truncated model approach close to the full order one. The error between the full order and corrected models is smaller at low frequencies and around 50 Hz it reaches a minimum value. As a result, model correction reduces the overall error due to model truncation, as desired.

In this study, the experimental system models based on displacement measurements were obtained by nonparametric identification. The smart beam was excited by piezoelectric patches with sinusoidal chirp signal of amplitude 5V within bandwidth of 0.1-60 Hz, which covers the first two flexural modes of the smart beam. The response of the smart beam was acquired via laser displacement sensor from specified measurement points. Since the patches are relatively thin compared to the passive aluminum beam, the system was considered as 1-D single input multi output system, where all the vibration modes are flexural modes. The open loop experimental setup is shown in Fig.7.

In order to have more accurate information about spatial characteristics of the smart beam, 17 different measurement points, shown in Fig.8, were specified. They are defined at 0.03m intervals from tip to the root of the smart beam.

The smart beam was actuated by applying voltage to the piezoelectric patches and the transverse displacements were measured at those locations. Since the smart beam is a spatially distributed system, that analysis resulted in 17 different single input single output system models where all the models were supposed to share the same poles. That kind of

analysis yields to determine uncertainty of resonance frequencies due to experimental approach. Besides, comparison of the analytical and experimental system models obtained for each measurement points was used to determine modal damping ratios and the uncertainties on them. That is the reason why measurement from multiple locations was employed. The rest of this section presents the comparison of the analytical and experimental system models to determine modal damping ratios and clarify the uncertainties on natural frequencies and modal damping ratios.

Consider the experimental frequency response of the smart beam at point $r = 0.99L_b$. Because experimental frequency analysis is based upon the exact dynamics of the smart beam, the values of the resonance frequencies determined from experimental identification were treated as being more accurate than the ones obtained analytically, where the analytical values are presented in Table 2. The first two resonance frequencies were extracted as 6.728 Hz and 41.433 Hz from experimental system model. Since the analytical and experimental models should share the same resonance frequencies in order to coincide in the frequency domain, the analytical model for the location $r = 0.99L_b$ was coerced to have the same resonance frequencies given above. Notice that, the corresponding measurement point can be selected from any of the measurement locations shown in Fig.8. Also note that, the analytical system model is the corrected model of the form given in equation (22). The resultant frequency responses are shown in Fig.9.

The analytical frequency response was obtained by considering the system as undamped. The point $r = 0.99L_b$ was selected as measurement point because of the fact that the free end displacement is significant enough for the laser displacement sensor measurements to be more reliable. After obtaining both experimental and analytical system models, the modal damping ratios were tuned until the magnitude of both frequency responses coincide at resonance frequencies, i.e.:

$$\left|G_E(s,r) - G_C(s,r)\right|_{\omega=\omega_i} < \lambda \tag{26}$$

where $G_E(s,r)$ is the experimental transfer function and λ is a very small constant term. Similar approach can be employed by minimizing the 2-norm of the differences of the displacements by using least square estimates (Reinelt, 2002).

Fig.10 shows the effect of tuning modal damping ratios on matching both system models in frequency domain where λ is taken as 10^{-6}. Note that each modal damping ratio can be tuned independently.

Consequently, the first two modal damping ratios were obtained as 0.0284 and 0.008, respectively. As the resonance frequencies and damping ratios are independent of the location of the measurement point, they were used to obtain the analytical system models of the smart beam for all measurement points. Afterwards, experimental system identification was again performed for each point and both system models were again compared in

frequency domain. The experimentally identified flexural resonance frequencies and modal damping ratios were determined by tuning for each point and finally a set of resonance frequencies and modal damping ratios were obtained. The amount of uncertainty on resonance frequencies and modal damping ratios can also be determined by spatial system identification. There are different methods which can be applied to determine the uncertainty and improve the values of the parameters ω and ξ such as boot-strapping (Reinelt, 2002). However, in this study the uncertainty is considered as the standard deviation of the parameters and the mean values are accepted as the final values, which are presented at Table 3.

	ω_1 (Hz)	ω_2 (Hz)	ξ_1	ξ_2
Mean	6.742	41.308	0.027	0.008
Standard Deviation	0.010	0.166	0.002	0.001

Table 3. Mean and standard deviation of the first two resonance frequencies and modal damping ratios

For more details about spatial system identification one may refer to (Kırcalı, 2006a).
The estimated and analytical first two mode shapes of the smart beam are given in Fig.11 and Fig.12, respectively (Kırcalı, 2006a).

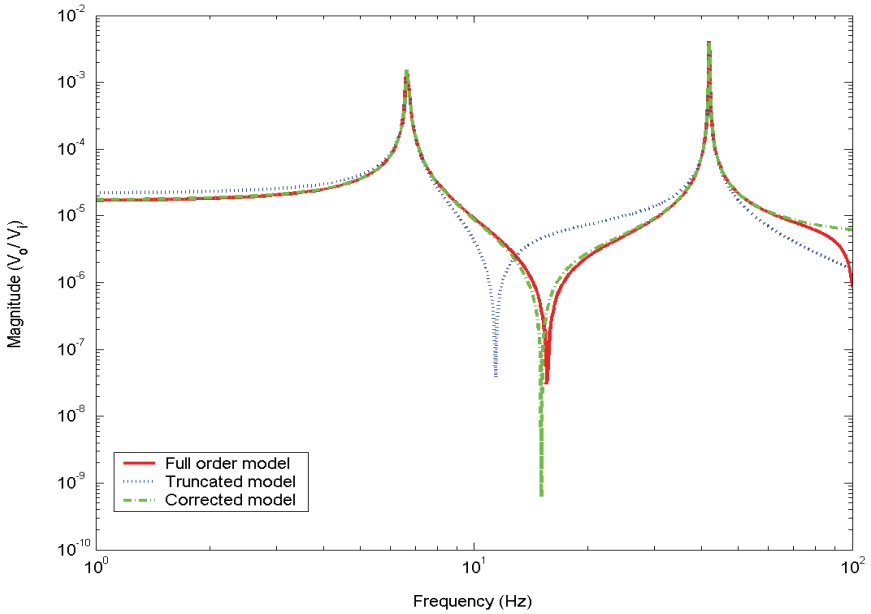

Fig. 3. Frequency response of the smart beam at $r = 0.14L_b$

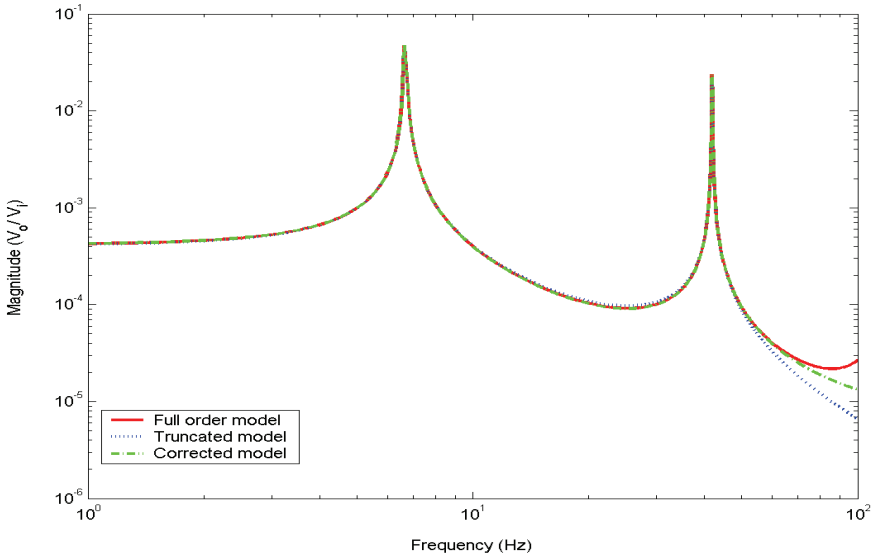

Fig. 4. Frequency response of the smart beam at $r = 0.99L_b$

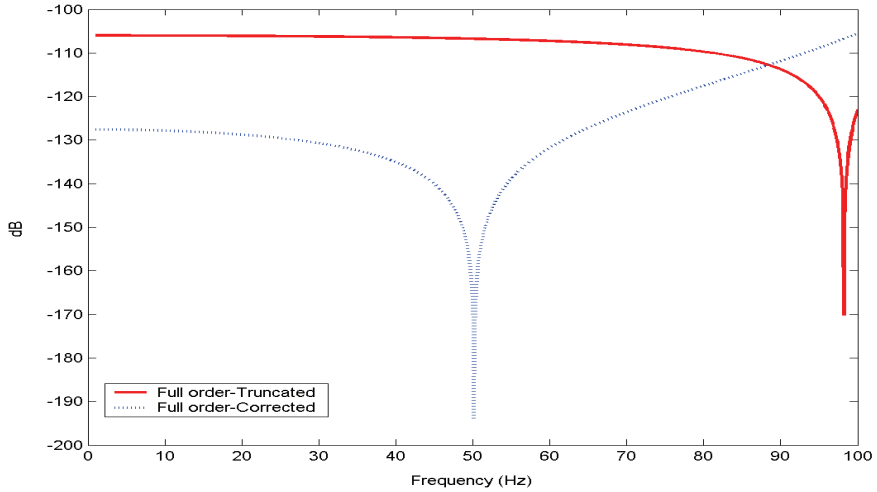

Fig. 5. Frequency responses of the error system models at $r = 0.14L_b$

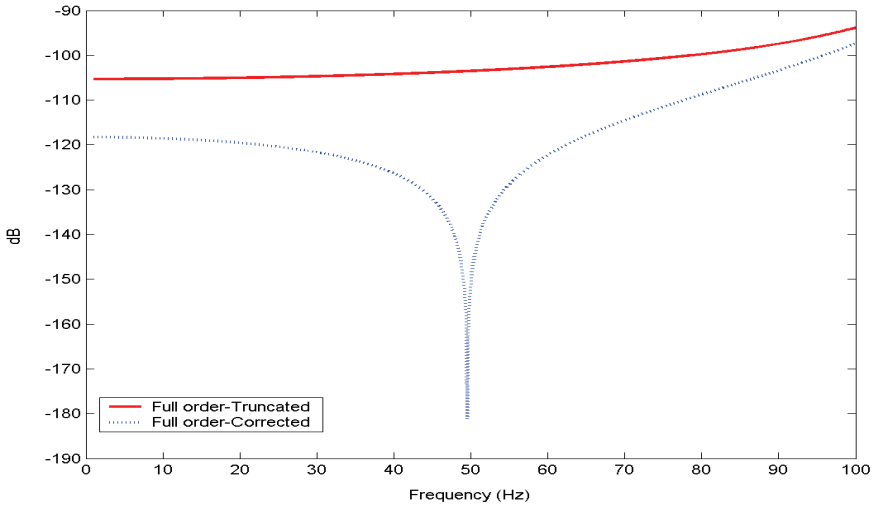

Fig. 6. Frequency responses of the error system models at $r = 0.99L_b$

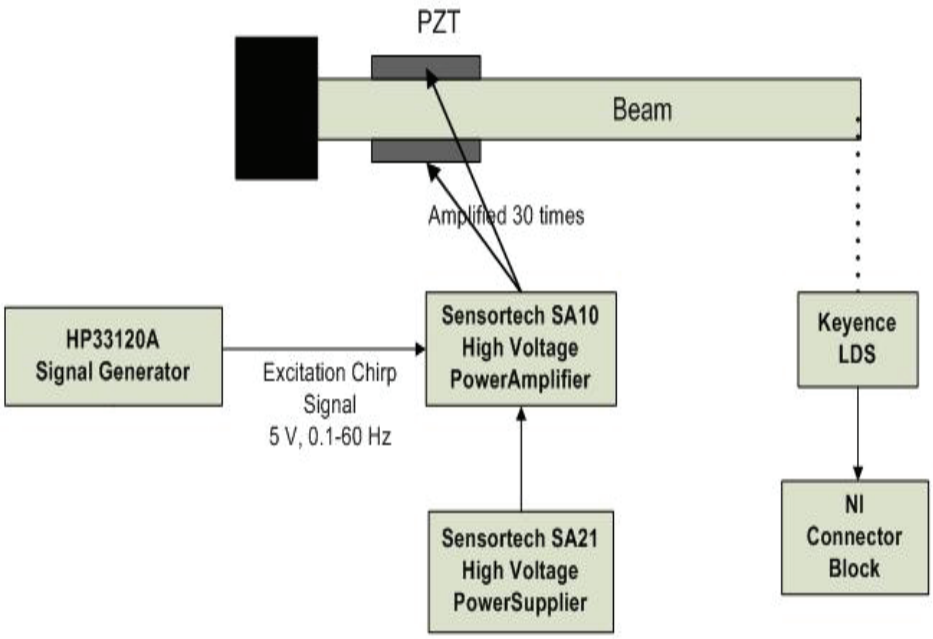

Fig. 7. Experimental setup for the spatial system identification of the smart beam

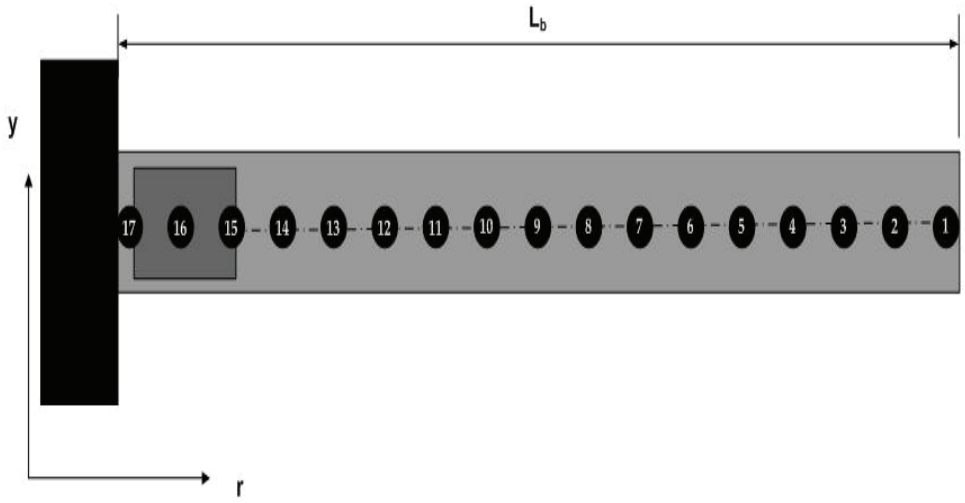

Fig. 8. The locations of the measurement points

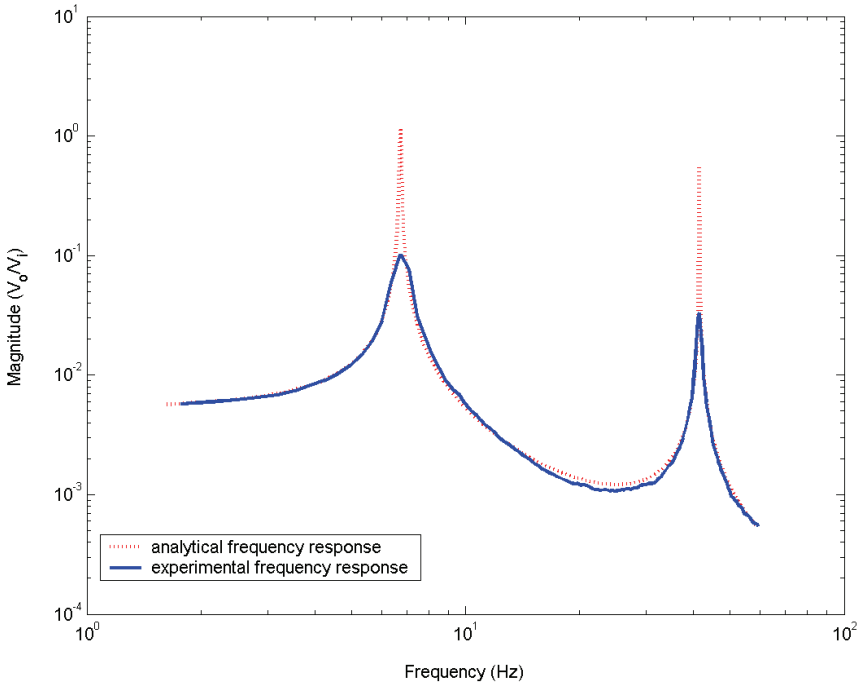

Fig. 9. Analytical and experimental frequency responses of the smart beam at r=0.99 L_b

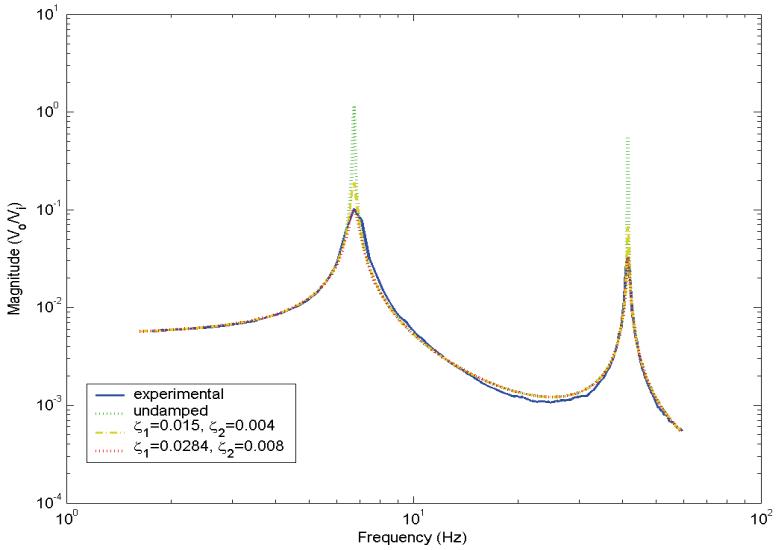

Fig. 10. Experimental and tuned analytical frequency responses at r=0.99 L_b

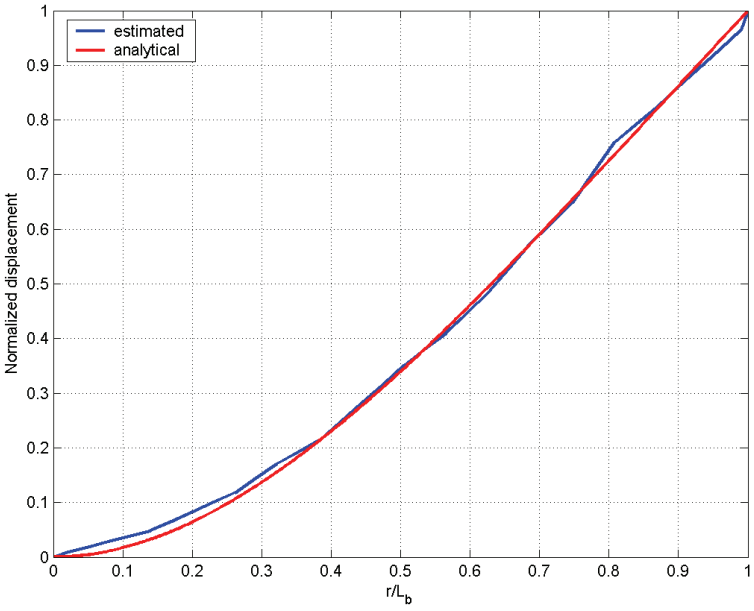

Fig. 11. First mode shape of the smart beam

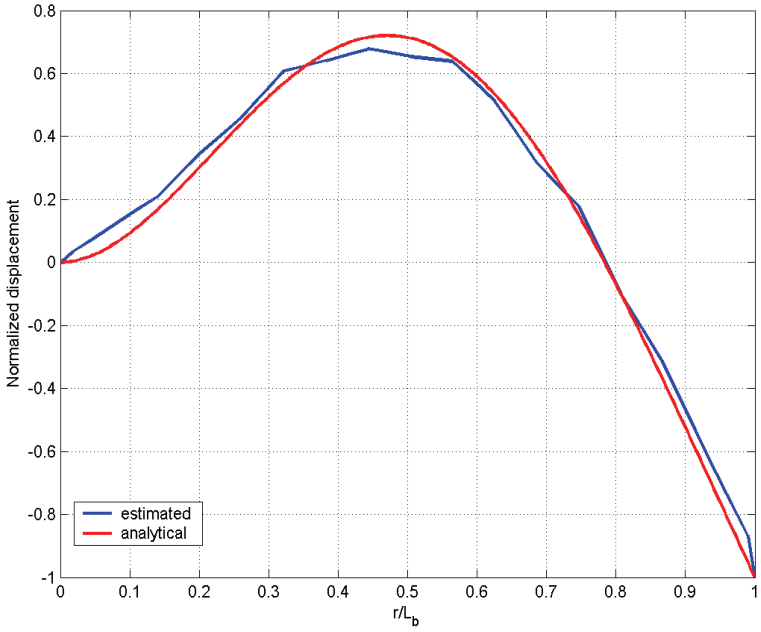

Fig. 12. Second mode shape of the smart beam

4. Spatial H_∞ Control Technique

Obtaining an accurate system model lets one to understand the system dynamics more clearly and gives him the opportunity to design a consistent controller. Various control design techniques have been developed for active vibration control like H_∞ or H_2 methods (Francis, 1984 and Doyle, 1989).

The effectiveness of H_∞ controller on suppressing the vibrations of a smart beam due to its first two flexural modes was studied by Yaman et al. (2001) and the experimental implementation of the controller was presented (2003). By means of H_∞ theory, an additive uncertainty weight was included to account for the effects of truncated high frequency modes as the model correction. Similar work has been done for suppressing the in-vacuo vibrations due to the first two modes of a smart fin (Yaman, 2002a, 2002b) and the effectiveness of the H_∞ control technique in the modeling of uncertainties was also shown.

However, H_∞ theory does not take into account the multiple sources of uncertainties, which yield unstructured uncertainty and increase controller conservativeness, at different locations of the plant. That problem can be handled by using the μ-synthesis control design method (Nalbantoğlu, 1998; Ülker, 2003 and Yaman, 2003).

Whichever the controller design technique is employed, the major objective of vibration control of a flexible structure is to suppress the vibrations of the first few modes on well-defined specific locations over the structure. As the flexible structures are distributed parameter systems, the vibration at a specific point is actually related to the vibration over the rest of the structure. As a remedy, minimizing the vibration over entire structure rather than at specific points should be the controller design criterion. The cost functions minimized as design criteria in standard H_2 or H_∞ control methodologies do not contain any information about the spatial nature of the system. In order to handle this absence, Moheimani and Fu (1998c), and Moheimani et al. (1997, 1998a) redefined H_2 and H_∞ norm concepts. They introduced spatial H_2 and spatial H_∞ norms of both signals and systems to be used as performance measures.

The concept of spatial control has been developed since the last decade. Moheimani et al. (1998a) studied the application of spatial LQG and H_∞ control technique for active vibration control of a cantilevered piezoelectric laminate beam. They presented simulation based results in their various works (1998a, 1998b, 1999). Experimental implementation of the spatial H_2 and H_∞ controllers were first achieved by Halim (2002a, 2002b, 2002c). These studies proved that the implementation of the spatial controllers on real systems is possible and that kind of controllers show considerable superiority compared to pointwise controllers on suppressing the vibration over entire structure. However, these works examined only simply-supported piezoelectric laminate beam. The contribution to the need of implementing spatial control technique on different systems was done by Lee (2005). Beside vibration suppression, he studied attenuation of acoustic noise due to structural vibration on a simply-supported piezoelectric laminate plate.

This section gives a brief explanation of the spatial H_∞ control technique based on the complete theory presented in reference (Moheimani, 2003). For more detailed explanation the reader is advised to refer to the references (Moheimani, 2003 and Halim, 2002b).

Consider the state space representation of a spatially distributed linear time-invariant (LTI) system:

$$\begin{aligned} \dot{x}(t) &= Ax(t) + B_1 w(t) + B_2 u(t) \\ z(t,r) &= C_1(r)x(t) + D_1(r)w(t) + D_2(r)u(t) \\ y(t) &= C_2 x(t) + D_3 w(t) + D_4 u(t) \end{aligned} \tag{27}$$

where r is the spatial coordinate, x is the state vector, w is the disturbance input, u is the control input, z is the performance output and y is the measured output. The state space representation variables are as follows: A is the state matrix, B_1 and B_2 are the input matrices from disturbance and control actuators, respectively, C_1 is the output matrix of

error signals, C_2 is the output matrix of sensor signals, D_1, D_2, D_3 and D_4 are the correction terms from disturbance actuator to error signal, control actuator to error signal, disturbance actuator to feedback sensor and control actuator to feedback sensor, respectively.

The spatial H_∞ control problem is to design a controller which is:

$$\begin{aligned} \dot{x}_k(t) &= A_k x_k(t) + B_k y(t) \\ u(t) &= C_k x_k(t) + D_k y(t) \end{aligned} \tag{28}$$

such that the closed loop system satisfies:

$$\inf_{K \in U} \ \sup_{w \in L_2[0,\infty)} J_\infty < \gamma^2 \tag{29}$$

where *U* is the set of all stabilizing controllers and γ is a constant. The spatial cost function to be minimized as the design criterion of spatial H_∞ control design technique is:

$$J_\infty = \frac{\int_0^\infty \int_R z(t,r)^T Q(r) z(t,r) dr dt}{\int_0^\infty w(t)^T w(t) dt} \tag{30}$$

where $Q(r)$ is a spatial weighting function that designates the region over which the effect of the disturbance is to be reduced. Since the numerator is the weighted spatial H_2 norm of the performance signal $z(t,r)$, J_∞ can be considered as the ratio of the spatial energy of the system output to that of the disturbance signal (Moheimani, 2003). The control problem is depicted in Fig.13:

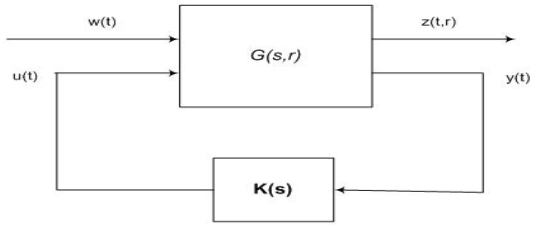

Fig. 13. Spatial H_∞ control problem

Spatial H_∞ control problem can be solved by the equivalent ordinary H_∞ problem (Moheimani, 2003) by taking:

$$\int_0^\infty \int_R z(t,r)^T Q(r) z(t,r) dr dt = \int_0^\infty \tilde{z}(t)^T \tilde{z}(t) dt \tag{31}$$

so, the spatial cost function becomes:

$$J_\infty = \frac{\int_0^\infty \tilde{z}(t)^T \tilde{z}(t) dt}{\int_0^\infty w(t)^T w(t) dt} \tag{32}$$

So the spatial H_∞ control problem is reduced to a standard H_∞ control problem for the following system:

$$\begin{aligned} \dot{x}(t) &= Ax(t) + B_1 w(t) + B_2 u(t) \\ \tilde{z}(t) &= \Pi x(t) + \Theta_1 w(t) + \Theta_2 u(t) \\ y(t) &= C_2 x(t) + D_3 w(t) + D_4 u(t) \end{aligned} \tag{33}$$

However, in order to limit the controller gain and avoid actuator saturation problem, a control weight should be added to the system.

$$\begin{aligned} \dot{x}(t) &= Ax(t) + B_1 w(t) + B_2 u(t) \\ \tilde{z}(t) &= \begin{bmatrix} \Pi \\ 0 \end{bmatrix} x(t) + \begin{bmatrix} \Theta_1 \\ 0 \end{bmatrix} w(t) + \begin{bmatrix} \Theta_2 \\ \kappa \end{bmatrix} u(t) \\ y(t) &= C_2 x(t) + D_3 w(t) + D_4 u(t) \end{aligned} \tag{34}$$

where κ is the control weight and it designates the level of vibration suppression. Control weight prevents the controller having excessive gain and smaller κ results in higher level of vibration suppression. However, optimal value of κ should be determined in order not to destabilize or neutrally stabilize the system.

Application of the above theory to our problem is as follows: Consider the closed loop system of the smart beam shown in Fig.14. The aim of the controller, K, is to reduce the effect of disturbance signal over the entire beam by the help of the PZT actuators.

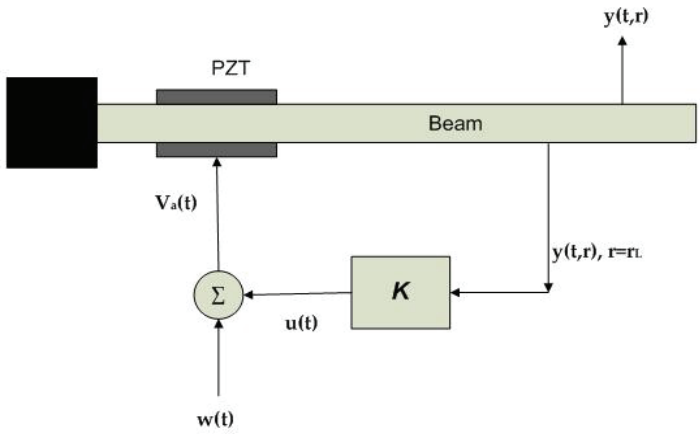

Fig. 14. The closed loop system of the smart beam

The state space representation of the system above can be shown to be (Kırcalı, 2008 and 2006a):

$$\begin{aligned} \dot{x}(t) &= Ax(t) + B_1 w(t) + B_2 u(t) \\ y(t,r) &= C_1(r)x(t) + D_1(r)w(t) + D_2(r)u(t) \\ y(t,r_L) &= C_2 x(t) + D_3 w(t) + D_4 u(t) \end{aligned} \tag{35}$$

where all the state space parameters were defined at Section 2.4, except the performance output and the measured output which are now denoted as $y(t,r)$ and $y(t,r_L)$, respectively. The performance output represents the displacement of the smart beam along its entire body, and the measured output represents the displacement of the smart beam at a specific location, i.e. $r = r_L$. The disturbance $w(t)$ is accepted to enter to the system through the actuator channels, hence, $B_1 = B_2$, $D_1(r) = D_2(r)$ and $D_3 = D_4$.

The state space form of the controller design, given in equation (28), can now be represented as:

$$\begin{aligned} \dot{x}_k(t) &= A_k x_k(t) + B_k y(t,r_L) \\ u(t) &= C_k x_k(t) + D_k y(t,r_L) \end{aligned} \tag{36}$$

Hence, the spatial H_∞ control problem can be represented as a block diagram which is given in Fig.15:

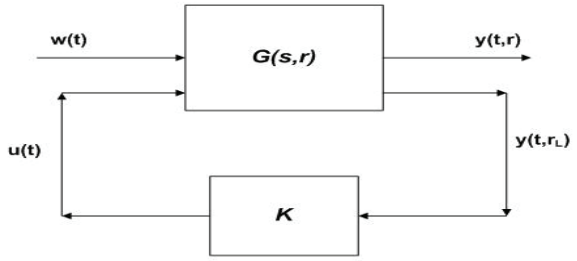

Fig. 15. The Spatial H_∞ control problem of the smart beam

As stated above, the spatial H_∞ control problem can be reduced to a standard H_∞ control problem. The state space representation given in equation (35) can be adapted for the smart beam model for a standard H_∞ control design as:

$$\begin{aligned} \dot{x}(t) &= Ax(t) + B_1 w(t) + B_2 u(t) \\ \tilde{y}(t) &= \begin{bmatrix} \Pi \\ 0 \end{bmatrix} x(t) + \begin{bmatrix} \Theta_1 \\ 0 \end{bmatrix} w(t) + \begin{bmatrix} \Theta_2 \\ \kappa \end{bmatrix} u(t) \\ y(t, r_L) &= C_2 x(t) + D_3 w(t) + D_4 u(t) \end{aligned} \tag{37}$$

The state space variables given in equations (35) and (37) can be obtained from the transfer function of equation (22) as:

$$A = \begin{bmatrix} 0 & 0 & 1 & 0 \\ 0 & 0 & 0 & 1 \\ -\omega_1^2 & 0 & -2\xi_1\omega_1 & 0 \\ 0 & -\omega_2^2 & 0 & -2\xi_2\omega_2 \end{bmatrix}, B_1 = B_2 = \begin{bmatrix} 0 \\ 0 \\ \overline{P}_1 \\ \overline{P}_2 \end{bmatrix} \tag{38}$$

$$\Pi = \begin{bmatrix} L_b^{3/2} & 0 & 0 & 0 \\ 0 & L_b^{3/2} & 0 & 0 \\ 0 & 0 & 0 & 0 \\ 0 & 0 & 0 & 0 \\ 0 & 0 & 0 & 0 \end{bmatrix}, \Theta_1 = \Theta_2 = \begin{bmatrix} 0 \\ 0 \\ 0 \\ 0 \\ \left(\sum_{i=3}^{50} L_b^3 \left(k_i^{opt} \right)^2 \right)^{1/2} \end{bmatrix} \tag{39}$$

$$C_1 = \begin{bmatrix} \phi_1(r) & \phi_2(r) & 0 & 0 \end{bmatrix}, C_2 = \begin{bmatrix} \phi_1(r_L) & \phi_2(r_L) & 0 & 0 \end{bmatrix} \tag{40}$$

$$D_1 = D_2 = \sum_{i=3}^{50} \phi_i(r) k_i^{opt}, D_3 = D_4 = \sum_{i=3}^{50} \phi_i(r_L) k_i^{opt} \tag{41}$$

The detailed derivation of the above parameters can be found in (Kırcalı, 2006a).

One should note that, in the absence of the control weight, κ, the major problem of designing an H_∞ controller for the system is that, such a design will result in a controller with an infinitely large gain (Moheimani, 1999). As previously described, in order to overcome this problem, an appropriate control weight, which is determined by the designer, is added to the system. Since the smaller κ will result in higher vibration suppression but larger controller gain, it should be determined optimally such that not only the gain of the controller does not cause implementation difficulties but also the suppression of the vibration levels are satisfactory. In this study, κ was taken as 7.87x10^{-7}.. The simulation of the effect of the controller is shown in Fig.16 as a bode plot. The frequency domain simulation was done by Matlab v6.5.

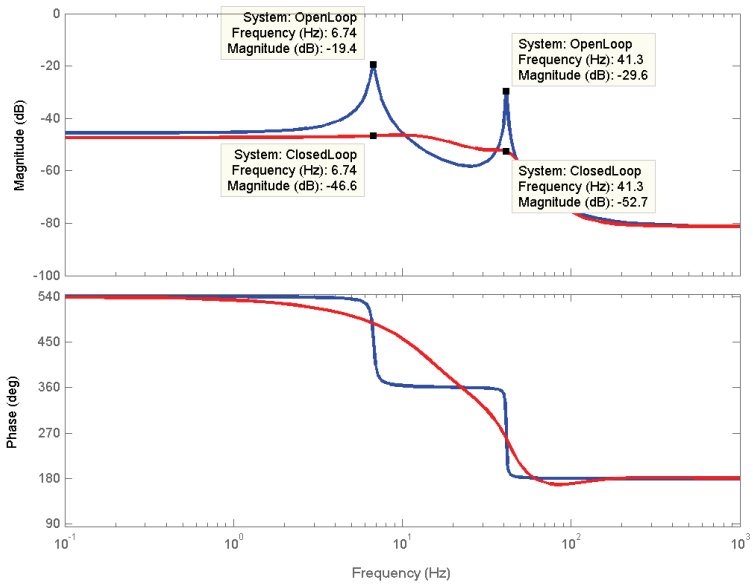

Fig. 16. Bode plots of the open loop and closed loop systems under the effect of spatial H_∞ controller

The vibration attenuation levels at the first two flexural resonance frequencies were found to be 27.2 dB and 23.1 dB, respectively. The simulated results show that the designed controller is effective on the suppression of undesired vibration levels.

4.1 Implementation of the Spatial Controller

This section presents the implementation of the spatial H_∞ controller for suppressing the free and forced vibrations of the smart beam. The closed loop experimental setup is shown in Fig.17. The displacement of the smart beam at a specific location was measured by using a Keyence Laser Displacement Sensor (LDS) and converted to a voltage output that was sent to the SensorTech SS10 controller unit via the connector block. The controller output was converted to the analog signal and amplified 30 times by SensorTech SA10 high voltage power amplifier before being applied to the piezoelectric patches. The controller unit is hosted by a Linux machine on which a shared disk drive is present to store the input/output data and the C programming language based executable code that is used for real-time signal processing.

For the free vibration control, the smart beam was given an initial 5 cm tip deflection and the open loop and closed loop time responses of the smart beam were measured. The results are presented in Fig.18 which shows that the controlled time response of the smart beam settles nearly in 1.7 seconds. Hence, the designed controller proves to be very effective on suppressing the free vibration of the smart beam.

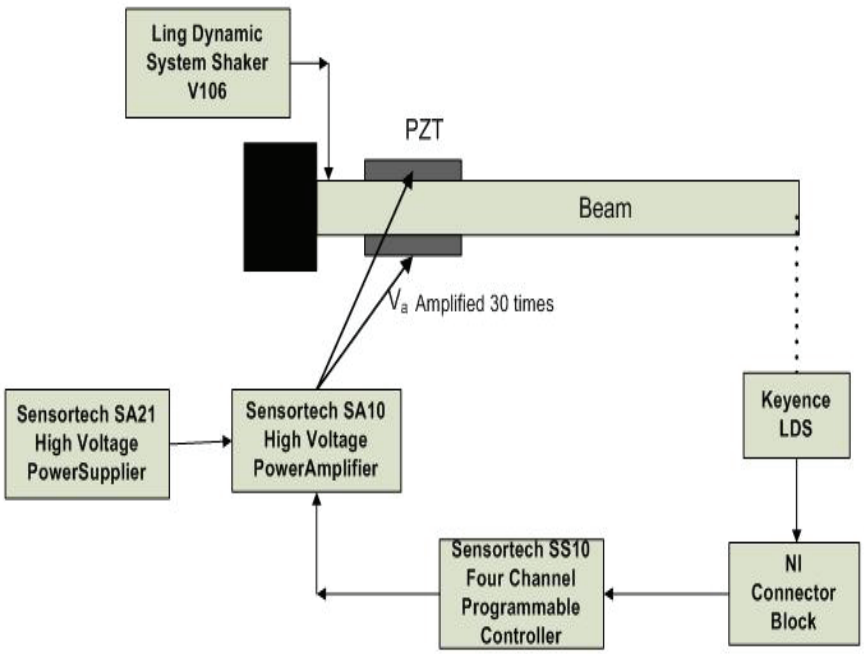

Fig. 17. The closed loop experimental setup

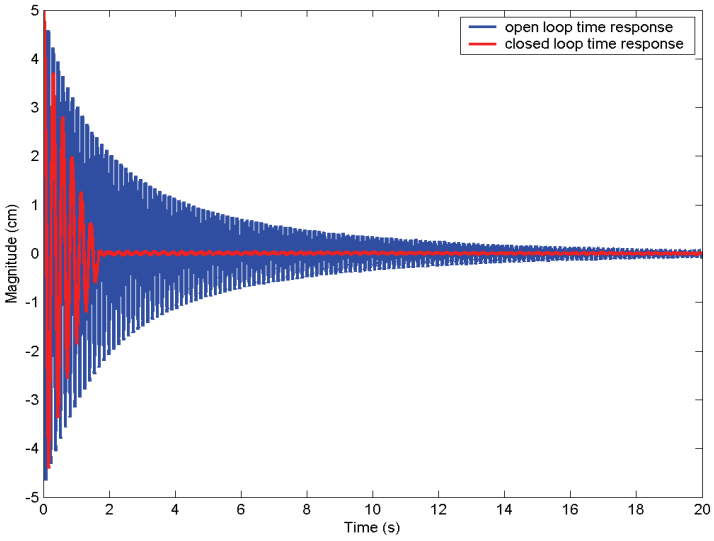

Fig. 18. Open and closed loop time responses of the smart beam under the effect of spatial H_∞ controller

The forced vibration control of the smart beam was analyzed in two different configurations. In the first one, the smart beam was excited for 180 seconds with a shaker located very close to the root of the smart beam, on which a sinusoidal chirp signal of amplitude 4.5V was applied. The excitation bandwidth was taken first 5 to 8 Hz and later 40 to 44 Hz to include the first two flexural resonance frequencies separately. The open loop and closed loop time and frequency responses of the smart beam under respective excitations are shown in Fig.19-a, Fig.19-b, Fig.20. Note that the Nyquist plot of the nominal system loop gain under the effect of spatial H_∞ controller given in Fig. 21 shows that the nominal system is stable.

The experimental attenuation of vibration levels at first two resonance frequencies were determined from the Bode magnitude plots of the frequency responses of the smart beam and shown in Fig.20-a and Fig.20-b. The resultant attenuation levels were found as 19.8 dB and 14.2 dB, respectively. Hence, the experimental results show that the controller is effective on suppression of the vibration levels. The reason why experimental attenuation levels are less than the simulated ones is that, the excitation power of the shaker was not enough to make the smart beam to reach the larger deflections which in turn causes a smaller magnitude of the open loop time response. The hardware constraints prevent one to apply higher voltages to the shaker. On the other hand, the magnitude of the experimental and simulated closed loop frequency responses at resonance frequencies being close to each other makes one to realize that, the controller works exactly according to the design criteria. Additionally, one should note that the attenuation levels were obtained from the decibel

magnitudes of the frequency responses. Hence, a simple mathematical manipulation can give the absolute attenuation levels as a ratio of the maximum time responses of the open and closed loop systems at the specified resonance frequencies.

In the second configuration, instead of using a sinusoidal chirp signal, constant excitation was applied for 20 seconds at the resonance frequencies with a mechanical shaker. The open loop and closed loop time responses of the smart beam were measured and shown in Fig.21 and Fig.22. Although, it is hard to control such a resonant excitation, the time responses show that the designed controller is still very effective on suppressing the vibration levels. Recall that the ratio of the maximum time responses of the open and closed loop systems can be considered as absolute attenuation levels; hence, for this case, the attenuation levels at each resonance frequency were calculated approximately as 10.4 and 4.17, respectively.

The robustness analysis of the designed controller was performed by Matlab v6.5 μ-synthesis toolbox. The results are presented in Fig. 23. The theoretical background of μ-synthesis is detailed in the References (Zhou, 1998 and Ülker, 2003). One should know that the μ values should be less than unity to accept the controllers to be robust. The Fig.23 shows that the spatial H_∞ controller is robust to the perturbations.

The efficiency of spatial controller in minimizing the overall vibration over the smart beam was compared by a pointwise controller that is designed to minimize the vibrations only at point $r = 0.99L_b$. For a more detailed description of the pointwise controller design, the interested reader may refer to the reference (Kırcalı, 2006a and 2006b). However, in order to give the idea of the previous studies, the comparative effects of the spatial and pointwise H_∞ controllers on suppressing the first two flexural vibrations of the smart beam are briefly presented in Table 4:

	Spatial H_∞ controller		Pointwise H_∞ controller	
Modes	1st mode	2nd mode	1st mode	2nd mode
Simulated attenuation levels (dB)	27.2	23.1	23.5	24.4
Experimentally obtained attenuation levels (dB)	19.8	14.2	21.02	21.66
Absolute attenuation levels under constant resonant excitation (max. OL time response/ max. CL time response)	10.4	4.17	5.75	4.37

Table 4. The comparison of attenuation levels under the effect of spatial and pointwise H_∞ controllers in forced vibrations

The simulations show that both controllers work efficiently on suppressing the vibration levels. The forced vibration control experiments of first configuration show that the attenuation levels of pointwise controller are slightly higher than those of the spatial one. Although the difference is not significant especially for the first flexural mode, better attenuation of pointwise controller would not be a surprise since the respective design criterion of a pointwise controller is to suppress the undesired vibration level at the specific measurement point. Additionally, absolute attenuation levels show that under constant resonant excitation at the first flexural mode, the spatial H_∞ controller has better performance than the pointwise one. This is because the design criterion of spatial controller is to suppress the vibration over entire beam; hence, the negative effect of the vibration at any point over the beam on the rest of the other points is prevented by spatial means. So, the spatial H_∞ controller resists more robustly to the constant resonant excitation than the pointwise one.

The implementations of the controllers showed that both controllers reduced the vibration levels of the smart beam due to its first two flexural modes in comparable efficiency (Kırcalı, 2006a and 2006b). The effect of both controllers on suppressing the first two flexural vibrations of the smart beam over entire structure can be analyzed by considering the H_∞ norm of the entire beam. Fig.24 shows the H_∞ norm plots of the smart beam as a function of *r* under the effect of both controllers.

5. General Conclusions

This study presented a different approach in active vibration control of a cantilevered smart beam.

The required mathematical modeling of the smart beam was conducted by using the assumed-modes method. This inevitably resulted in a higher order model including a large number of resonant modes of the beam. This higher order model was truncated to a lower model by including only the first two flexural vibrational modes of the smart beam. The possible error due to that model truncation was compensated by employing a model correction technique which considered the addition of a correction term that consequently minimized the weighted spatial H_2 norm of the truncation error. Hence, the effect of out-of-range modes on the dynamics of the system was included by the correction term. During the modeling phase the effect of piezoelectric patches was also conveniently included in the model to increase the accuracy of the system model. However, the assumed-modes modeling alone does not provide any information about the damping of the system. It was shown that experimental system identification, when used in collaboration with the analytical model, helps one to obtain more accurate spatial characteristics of the structure. Since the smart beam is a spatially distributed structure, experimental system identification based on several measurement locations along the beam results in a number of system models providing the spatial nature of the beam. Comparison of each experimental and analytical system models in the frequency domain yields a significant improvement on the determination of the natural frequencies and helps one to identify the uncertainty on them.

Also, tuning the modal damping ratios until the magnitude of both frequency responses coincide at resonance frequencies gives valid damping values and the corresponding uncertainty for each modal damping ratio.

This study also presented the active vibration control of the smart beam. A spatial H_∞ controller was designed for suppressing the first two flexural vibrations of the smart beam. The efficiency of the controller was demonstrated both by simulations and experimental implementation. The effectiveness of spatial controller on suppressing the vibrations of the smart beam over its entire body was also compared with a pointwise one.

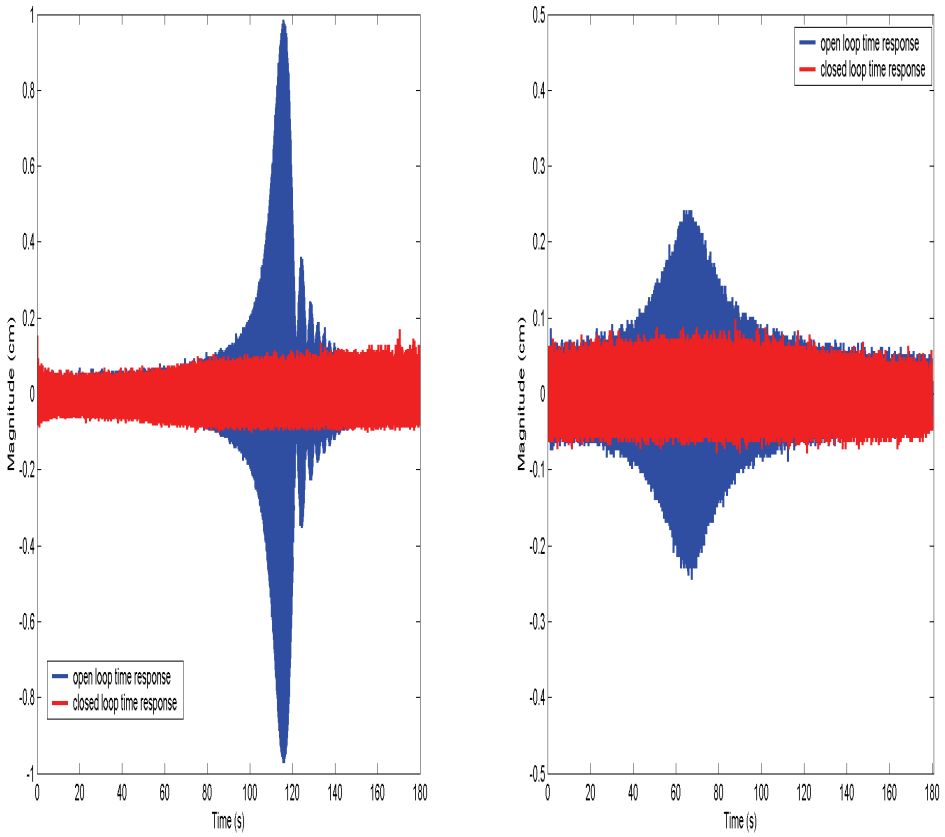

a) Within excitation of 5-8 Hz

b) Within excitation of 40-44 Hz

Fig. 19. Time responses of the smart beam

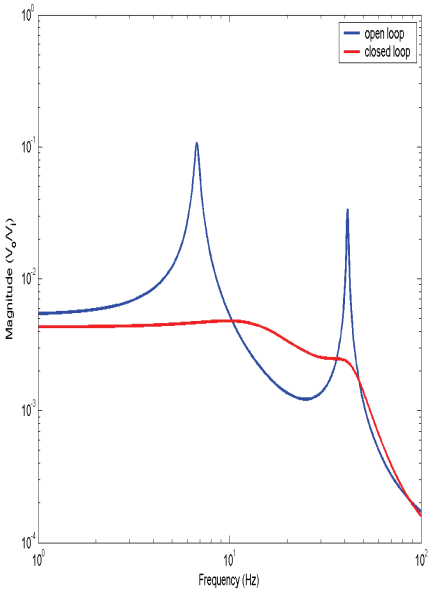

Fig. 20. Open and closed loop frequency responses of the smart beam

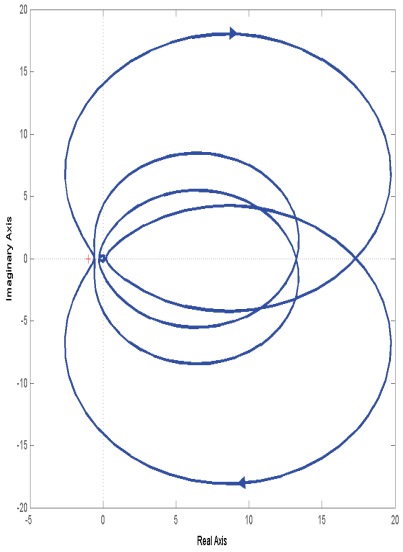

Fig. 21. Nyquist plot

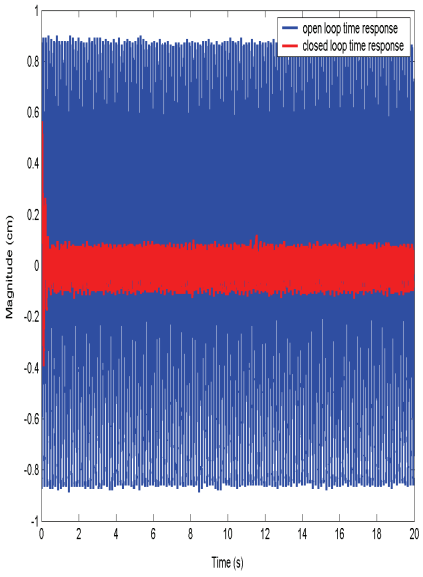

Fig. 21. Open and closed loop time responses at first resonance frequency

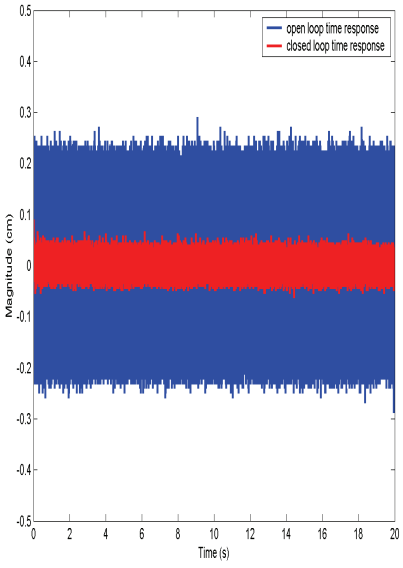

Fig. 22. Open and closed loop time responses at second resonance frequency

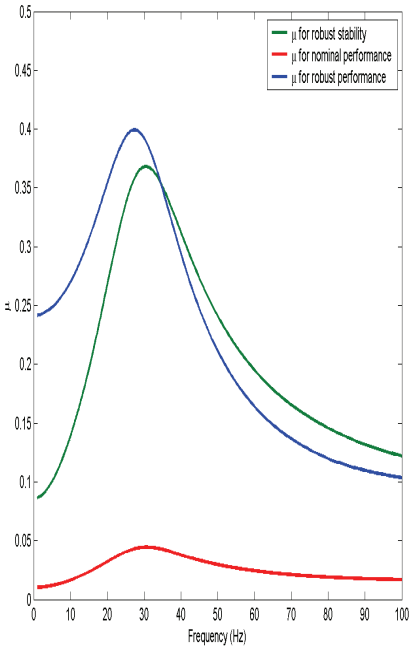

Fig. 23. μ-analysis for spatial H_∞ controller

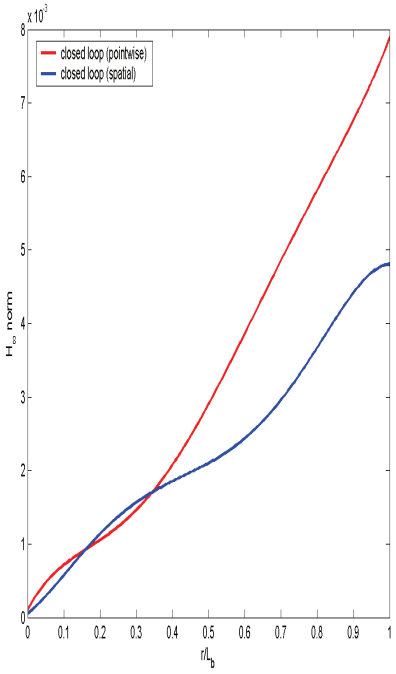

Fig. 24. Simulated H_∞ norm plots of closed loop systems under the effect of pointwise and spatial H_∞ controllers

6. References

Bai M., Lin G. M., (1996). The Development of DSP-Based Active Small Amplitude Vibration Control System for Flexible Beams by Using the LQG Algorithms and Intelligent Materials, *Journal of Sound and Vibration*, 198, Vol. 4, pp. 411-427.

Balas G., Young P. M., (1995). Control Design For Variations in Structural Natural Frequencies, *Journal of Guidance, Control and Dynamics*, Vol. 18, No. 2.

Baz A., Poh S., (1988). Performance of an Active Control System with Piezoelectric Actuators, *Journal of Sound and Vibration*, 126(2), pp. 327-343.

Clark R.L., (1997). Accounting for Out-of-Bandwidth Modes in the Assumed Modes Approach: Implications on Colocated Output Feedback Control, *Transactions of the ASME, Journal of Dynamic Systems, Measurement, and Control*, Vol. 119, pp. 390-395.

Crawley E.F., Louis J., (1989). Use of Piezoelectric Actuators as Elements of Intelligent Structures, *AIAA Journal*, Vol. 125, No. 10, pp. 1373-1385

Çalışkan T., (2002). *Smart Materials and Their Applications in Aerospace Structures*, PhD Thesis, Middle East Technical University.

Dimitridis E.K.C., Fuller R., Rogers C. A., (1991). Piezoelectric Actuators for Distributed Vibration Excitation of Thin Plates, *Journal of Vibration and Acoustics*, Vol. 113, pp. 100-107.

Doyle J. C., Glover K., Khargonekar P.P., Francis B. A., (1989). State-Space Solutions to Standard and Control Problems, *IEEE Transactions on Automatic Control*, 34(8), pp. 831-847.

Francis B. A., Zames G., (1984). On Optimal Sensitivity Theory for SISO Feedback Systems, *IEEE Transactions on Automatic Control*, Vol. AC-29, No.1.

Gosavi S.V., Kelkar A.G., (2004). Passivity-Based Robust Control of Piezo-Actuated Flexible Beam, *Journal of Vibration and Acoustics*, Vol. 126, pp. 260-271.

Halim D., Moheimani S.O.R., (2002a). Experimental Implementation of Spatial Control on a Piezoelectric Laminate Beam, *IEEE/ASME Transactions on Mechatronics*, Vol. 7, No:3.

Halim D.,, (2002b). *Vibration Analysis and Control of Smart Structures*, PhD. Thesis, School of Electrical Engineering and Computer Science, University of Newcastle, Australia.

Halim D., Moheimani S.O.R., (2002c). Spatial Control of a Piezoelectric Laminate Beam: Experimental Implementation, *IEEE Transactions on Control System Technology*, Vol. 10, No:4

Hanagoud S., Obal M. W., Calise A. J., (1992). Optimal Vibration Control by the Use of Piezoceramic Sensors and Actuators, *Journal of Guidance, Control and Dynamics*, Vol. 15, No. 5, pp. 1199-1206.

Hughes P.C., (1987). Space Structure Vibration Modes: How Many Exist? Which Ones Are Important?, *IEEE Control Systems Magazine*, pp. 22-28.

Hughes P.C., Skelton R.E., (1981). Modal Truncation for Flexible Spacecraft, *Journal of Guidance and Control*, Vol. 4, No.3.

Kırcalı Ö.F., Yaman Y., Nalbantoğlu V., Şahin M., Karadal F.M, (2008). Spatial Control of a Smart Beam, *Journal of Electroceramics*, 20(3-4): 175-185

Kırcalı Ö.F., Yaman Y., Nalbantoğlu V., Şahin M., Karadal F.M., (2007). Application of Spatial H∞ Control Technique for Active Vibration Control of a Smart Beam, *ICINCO 2007, International Conference on Informatics in Control, Automation and Robotics*, Paper C3-425, Angers, France

Kırcalı Ö.F., (2006a). *Active Vibration Control of a Smart Beam: A Spatial Approach*, M.S. Thesis, Middle East Technical University.

Kırcalı Ö.F., Yaman Y., Nalbantoğlu V., Şahin M., Karadal F.M., (2006b). Comparison of Spatial and Pointwise Controllers in Vibration Control of a Smart Beam, *I. National Aerospace Symposium*, METU, Ankara, Turkey (in Turkish)

Lee Y.K., (2005). *Active Vibration Control of a Piezoelectric Laminate Plate Using Spatial Control Approach*, M.S. Thesis, Department of Mechanical Engineering, University of Adelaide, Australia

Lenz K., Özbay H., (1993). Analysis and Robust Control Techniques for an Ideal Flexible Beam, *Control and Dynamic Systems*, 57: 369-421

Ljung L., (1987). *System Identification: Theory for the User*, Prentice-Hall.

Mason W.P., (1981). Piezoelectricity, its History and Applications, *Journal of Acoustical Society of America*, Vol. 70, No. 6

Meirovitch L., (1986). *Elements of Vibration Analysis*, The McGraw-Hill Company

Moheimani S.O.R., Halim D., Fleming A.J., (2003). *Spatial Control of Vibration. Theory and Experiments*, World Scientific Publishing Co. Pte. Ltd.

Moheimani S.O.R., (2000a). Minimizing the Effect of Out-of-Bandwidth Dynamics in the Models of Reverberant Systems That Arise in Modal Analysis: Implications on Spatial Control, *Automatica*, Vol. 36, pp. 1023-1031

Moheimani S.O.R., (2006b). Experimental Verification of the Corrected Transfer Function of a Piezoelectric Laminate Beam, *IEEE Transactions on Control Systems Technology*, Vol. 8, No. 4, pp. 660-666

Moheimani S.O.R., Clark R.L., (2000c). Minimizing the Truncation Error in Assumed Modes Models of Structures, *Transactions of the ASME, Journal of Vibration and Acoustics*, Vol. 122, pp.332-335

Moheimani S.O.R., (2000d). Minimizing the Effect of out of Bandwidth Modes in Truncated Structure Models, *Transactions of the ASME, Journal of Dynamic Systems, Measurement, and Control*, Vol. 122, pp.237-239

Moheimani S.O.R., Petersen I.R., Pota H.R., (1999). Broadband Disturbance Attenuation over an Entire Beam, *Journal of Sound and Vibration*, 227(4): 807-832

Moheimani S.O.R., Pota H.R., Petersen I.R., (1998a). Spatial Control for Active Vibration Control of Piezoelectric Laminates, *International Proceedings of 37th IEEE CDC*, Tampa, Florida, USA, December 1998

Moheimani S.O.R., Pota H.R., Petersen I.R., (1998b). Active Control of Noise and Vibration in Acoustic Ducts and Flexible Structures – a Spatial Control Approach, *Proceedings of ACC*, Philadelphia, Pennsylvania, USA, June 1998

Moheimani S.O.R, Fu M., (1998c). Spatial Norm of Flexible Structures and its Application in Model Order Selection, *International Proceedings of 37th IEEE Conference on Decision and Control*, Tampa Florida, USA, 1998

Moheimani S.O.R., Pota H.R., Petersen I.R., (1997). Spatial Balanced Model Reduction for Flexible Structures, *Proceedings of the American Control Conference*, pp. 3098-3102, Albuquerque, New Mexico, June 1997

Nalbantoğlu V., Bokor J., Balas G., Gaspar P., (2003). System Identification with Generalized Orthonormal Basis Functions: an Application to Flexible Structures, *Control Engineering Practice* , Vol. 11, pp.245-259

Nalbantoğlu V., (1998). *Robust Control and System Identification for Flexible Structures*, Ph. D. Thesis, University of Minnesota

Pota H.R., Alberts T.E., (1992). Multivariable Transfer Functions for a Slewing Piezoelectric Laminate Beam, *Proceedings IEEE International Conference on Systems Engineering*, Japan, September 1992

Prasad S.E., Ahmad A., Wheat T.A., (1998). The Role of Smart Structures in Robotics, *Canada-US CanSmart Workshop on Smart Materials and Structures*, Quebec, Canada Proceedings pp:133-147, 1998

Reinelt W., Moheimani S.O.R., (2002). Identification of a Flexible Beam, *In Proceedings of the 8th International Mechatronics Conference*, Enschede, Netherlands, 2002

Ülker F.D., (2003). *Active Vibration Control of Smart Structures*, M.S. Thesis, Middle East Technical University

Yaman Y., Ülker F.D., Nalbantoğlu V.,Çalışkan T., Prasad E., Waechter D., Yan B., (2003a). Application of μ-Synthesis Active Vibration Control Technique to a Smart Fin, *6th CanSmart, International Workshop on Smart Materials and Structures*, Montreal, Canada Proceedings pp:109-118, 2003

Yaman Y., Ülker F. D., Nalbantoğlu V., Çalışkan T., Prasad E., Waechter D., Yan B., (2003b). Application of Active Vibration Control Strategy in Smart Structures, *AED2003, 3rd International Conference on Advanced Engineering Design*, Paper A5.3, Prague, Czech Republic, 01-04 June, 2003

Yaman Y., Çalışkan T., Nalbantoğlu V., Prasad E., Waechter D., (2002a). Active Vibration Control of a Smart Plate, *ICAS2002, International Council of the Aeronautical Sciences*, Paper 424, Toronto, Canada, September 8-13, 2002

Yaman Y., Çalışkan T., Nalbantoğlu V., Ülker F. D., Prasad E., Waechter D., Yan B., (2002b). Active Vibration Control of Smart Plates by Using Piezoelectric Actuators, *ESDA2002, 6th Biennial Conference on Engineering Systems Design and Analysis*, Paper APM-018, Istanbul, Turkey, July 8-11, 2002

Yaman Y., Çalışkan T., Nalbantoğlu V., Prasad E., Waechter D., Yan B., (2001). Active Vibration Control of a Smart Beam, *Canada-US CanSmart Workshop on Smart Materials and Structures*, Montreal, Canada Proceedings pp:137-147, 2001

Zames G., (1981). Feedback and Optimal Sensitivity: Model Reference Transformations, Multiplicative Seminorms, and Approximate Inverses, *IEEE Transactions on Automatic Control*, Vol. AC-26, No.2, April 1981

Zhou G., Doyle J.C., (1998). *Essentials of Robust Control*, Prentice-Hall